

Analysis of the Relationship Between Urban Land Use and Urban Heat Island Using Remote Sensing Methods

László MUCSI¹, László HENITS, and János UNGER
University of Szeged, Hungary

Abstract. Remote sensing has considerable potential for providing accurate, up-to-date information in urban areas. Urban remote sensing is complicated, however, by very high spectral and spatial complexity. In this paper, beside traditional per-pixel method (annual NDVI change detection using Landsat TM images), Normalized Endmember Spectral Mixture Analysis (NSMA) was applied to map urban land cover. The TM images were acquired over the city of Szeged, Hungary in 1986 and 2009. The urban land use categories were classified according to the standard deviation (SD) of NDVI values of 8 TM images in 1986. Significant linear connection was calculated between the SD values and the sub-pixel rate of impervious surfaces. Impervious surface, one of the most important elements of the VIS model, has been recognized as a key indicator in assessing of the change of the urban environment in the last 25 years in the city. The spatial statistical analysis of internal land use change was developed on the traditional urban zones. Later, the urban land cover map was the main database for the estimation of spatial distribution of urban heat island. The result of the geostatistical analysis demonstrated a very strong connection between urban land cover classes and spatial characteristics of urban heat island..

Keywords. urban land use, urban heat island, spectral mixture analysis, standard deviation of NDVI

Introduction

Time series vegetation indices (VI), just like NDVI or EVI are traditionally made from the records produced by satellite sensors with low temporal resolution (NOAA AVHRR, MERIS, SPOT VEGETATION, MODIS, etc.) and can be taken in global scale, even day-to-day as well. Development of an effective analysis upon the time series data is an important question of the remote sensing [Bruzzone et al., 2003]. Especially the data series of the NDVI have great importance in the phenological analysis of plants and in the numerical observation of vegetation growth [Hall-Beyer, 2003; Petorelli et al. 2005]. In Hungary vegetation indices were used to analyse urban surfaces since the beginning of the 90's [Mezosi and Mucsi, 1994; Unger J, 1999; Unger et al. 2001; Mucsi et al., 2007], especially after proving that NDVI is one of the best indicators of urban climate. Close connection can be established the NDVI values of urban and rural areas and the minimum air and surface temperature [Gallo et al, 1993]. We can derive and evaluate important parametres of the urban climate model from the relation of NDVI values and the land surface temperature (LST), such as the ratio factor of the vegetation coverage or soil moisture [Gillies and Carlson, 1995; Gillies et al, 1997].

Higher NDVI values are indicators of vegetation coverage inside the cell. Vegetation affects the latent thermoflux of the surface intent to the atmosphere through the evapotranspiration. Lower LST (except water bodies) is usually measured in areas with higher NDVI values. This negative correlation between NDVI and LST is an important result of urban climate research. However, growth of vegetation causes the seasonal change of NDVI values, hence its connection to urban LST and to

¹ Corresponding Author. László MUCSI, associate professor, University of Szeged, Hungary, Dept. of Physical Geography and Geoinformatics, email: mucsi@geo.u-szeged.hu, address: H-6725 Szeged, Egyetem str. 2-6, POB: 653

the formation and extent of urban heat islands shows also a seasonal difference. This connection between NDVI and LST values is nonlinear and the temperature over bare soil surfaces represent much more variability than the temperature over surfaces covered by dense vegetation [Carlson et al. 1994; Gillies and Carlson, 1995; Owen et al. 1998]. Variability and the nonlinear relation assumes, that only NDVI alone may not be a sufficient metric to analyse urban heat island index quantitatively. Weng et al. [2004] proposed to use vegetation coverage ratio factor derived from Spectral Mixture Analysis of pixels as a new indicator instead of NDVI values. They found out that this factor has a slightly stronger negative correlation with the temperature of surface than NDVI has. Although the production of vegetation coverage ratio factor differs from NDVI, it can still be settled as a vegetation index, which has a close correlation to NDVI values [Carlson and Ripley, 1997].

According to the aforementioned, in case of urban areas the pixel-based definition of artificial or vegetation-covered surfaces is possible only if the spatial resolution of the applied sensor reaches, or at least approaches the spatial scale of urban reflectance. However, this value can vary in different cities or in the differently built-up parts of a city. According to our previous studies [Henits, 2007] in Szeged (Hungary) this scale varies between 10 and 60 metres, hence Landsat or SPOT images might be appropriate to calculate cell-based NDVI values, especially if we manage to derive a parameter from these images that refers to the territorial rate of the main land cover types inside the pixel.

A single satellite image is not enough to state, in the certain time what the relation between NDVI values and land cover is, and the condition of the vegetation and the former climatic circumstances (precipitation and temperature changes) determine the NDVI. Middle-scale sensors are not capable to monitor the vegetation because of their longer temporal resolution (16-27 days). However, in fortunate case the database contains images, able for series analysis, which are free from clouds and show the actual state of land cover more times during the phenological period of urban vegetation inside the cities and in the surroundings. After collecting these images we have the chance to calculate such statistical parameters from single NDVI maps, that integrate differences of seasonal changes in the urban area and we are able to analyse the relation between these parameters and the built-up density calculated from other sources or the relation with the values of heat island intensity.

1. Used data and preprocessing

In our research we were keen to collect as many images as available from the same year, with the widest range of time interval, produced by the same sensor (Landsat TM). Landsat-5 satellites provide cover every 16 days from the same area, so the time-lag between the temporal closest images is at least 16 days long. However, several times we couldn't manage to use the next image in the order, because cloud cover made them inappropriate for scientific analysis.

The satellite images were downloaded from the internet database (<http://glovis.usgs.gov>) of the U.S. Geological Survey (USGS). We found 8 pieces of Landsat-5 TM images for the location of Szeged, Hungary in the year of 1986 (16th April, 2nd and 18th May, 19th June, 5th July, 22nd August, 7th September, 25th October) which fit to all conditions described below. Each of the images were transformed into the UTM projection system (WGS84 ellipsoid, zone 34). From the following years we couldn't download records in such big amount or in or in such a good quality (free from cloud cover). For the validation we used a Landsat TM image from the 24th July 1987.

The intensity values of Landsat-5 TM were transformed to reflectance values using atmospheric correction, consuming a model created in ERDAS IMAGINE [Chavez, 1996, Chander and Markham, 2003].

For each bands of the image the theoretical radiation value of black body was calculated, which can be assumed as 1% of the reflectance [Chavez, 1996; Moran et al., 1992].

2. Methods and the results

NDVI is one of the most widely used vegetation index of which applicability in satellite analysis and in monitoring of vegetation cover was sufficiently verified in the last two decades[Liu and Huete, 1994; Leprieur et al., 2000]. It has the following formula:

$$NDVI = \frac{NIR - R}{NIR + R}$$

where NIR means the near infrared reflectance of the surface and R is the one of the red band. The value of the pixels varies between -1 and +1, the higher it is, the richer and more healthy the vegetation is.

When analysing single image NDVI values it is often raised, in the case of homogeneous vegetal clouds should these values be interpreted as the resultant of previous, dynamically changing climate (precipitation, air temperature) or of other, static circumstances (e.g. properties of the soil). Also in the case of spectral mixed pixels it is obvious that, depending on the season, artificial surfaces are differently covered by canopy and that in the growing season the growth of vegetation takes effect on the result of sub-pixel-based analysis of spectral mixed pixels (e.g. SMA, the Spectral Mixture Analysis) and on the endmember rate map values. We assume that if we could describe the interim changes of NDVI values with statistical parameter, then we could dissolve the stationarity of NDVI maps recorded in one single time, and these new parameter could be useful to map land cover also at urban surfaces where middle-scale satellite images contain also spectral mixed pixels.

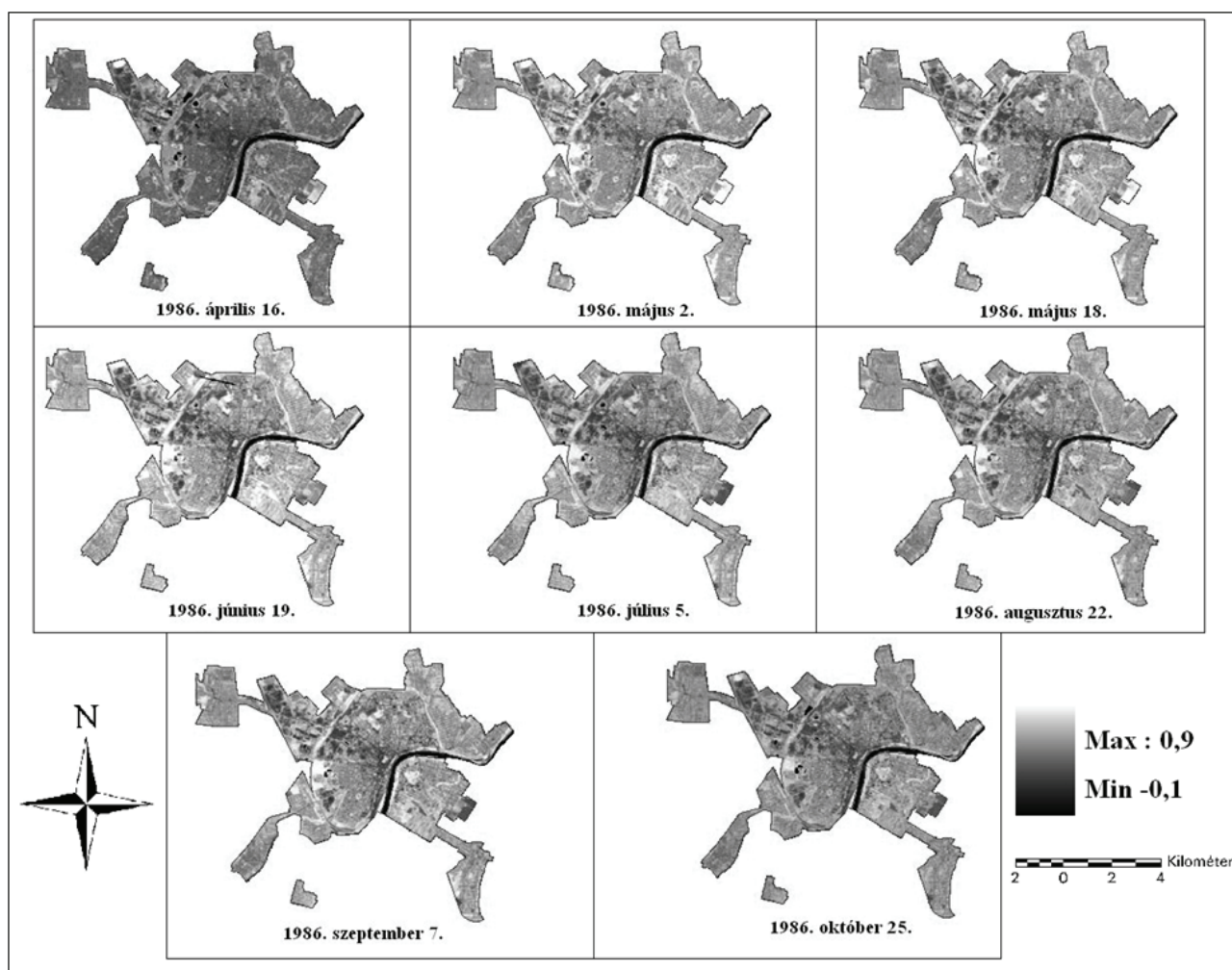


Figure 1. NDVI images produced from Landsat TM satellite images

After analysing the Landsat TM satellite images which cover the whole growing season of 1986 (comparison by pixels, differencing, statistical analysis) we established that (Figure 1, Figure 2) that the interim changes of NDVI values are much smaller in the case of the selected pixels which contain mainly homogeneous artificial surfaces (0,14-0,24), than in the case of cells that cover vegetal clouds (0,65-0,72). Although only 8 images were available from the growing season to calculate NDVI values with, and it is unadvisable to conjugate the values fixed to discrete moments with a continuous line in the graphical representation, but its still a rare opportunity to calculate NDVI values from so many measured data (images free from clouds). This use was later confirmed again when Landsat TM images, which cover Szeged and have the ID 186-028 (their times of record bisect the 16 days long periods of temporal resolution of the analysed TM images with ID 187-028) gave such NDVI values as a result that fitted exactly to the diagram represented in the Fig.1. In urban areas covered with vegetation NDVI values were increasing continuously between April and the middle of June. After that they were decreasing because of the hot and dry weather, then, at the end of July, they approached the values measured in the middle of June. After the local max of September NDVI values tended to decrease until the end of October, the end of the phenological period of the vegetation, practically until the record of the last, cloud-free autumn image. To this time, the canopy of deciduous trees started to rarefy and the decline of the canopy's chlorophyll content became notable.

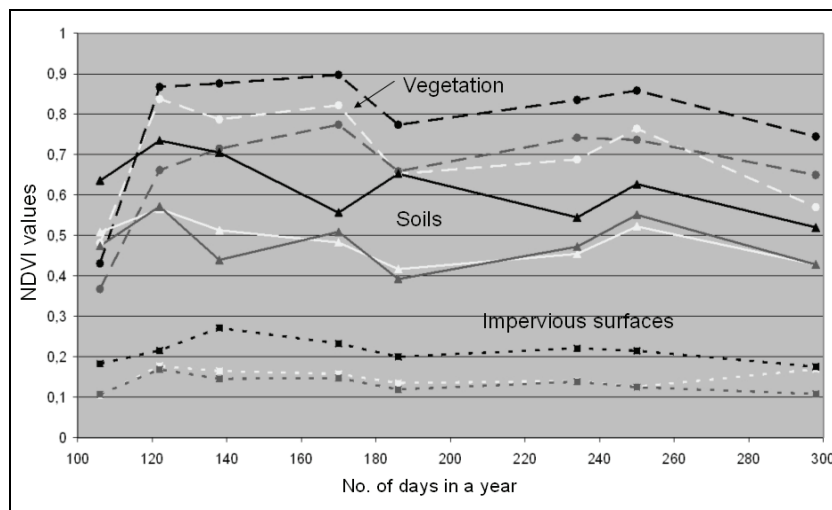


Figure 2. NDVI changes of representative urban land cover types (artificial surface, vegetation, soil) in 1986

After the statistical analysis of NDVI values we could state that standard deviation values significantly differ in cases of certain land cover types and might relate to the built-up density. Also according to the table and the diagrams it is found that the interim standard deviation of artificial surfaces is rather low ($\sigma=0.02-0.03$), vegetation has higher values ($\sigma>0.13$) and the deviation values of urban soil surface are between two of them ($\sigma=0.05-0.08$).

Hence we created the deviation map of the total settlement area, based on 8 input NDVI images (Figure 3). As a result we obtained deviation values from the examined year for each pixel.

We illustrated also the spatial distribution of deviation values calculated from 8 NDVI values per pixel. The following properties of the NDVI deviation map prove the close relationship between deviation and built-up density:

1. inner, well built-up parts of the city and the coherent industrial buildings of the east-west axle, marked with bright colour are easy to recognise,
2. traditional suburbs with lower built-up density are marked with grey (eastern, southern and northern parts of Szeged: Alsóváros, Móraváros, Rókus),
3. smaller, dark blurs indicate parks, cemeteries, the forest around the embankment of Szeged, scrublands and all the gardens and agricultural land around the city.

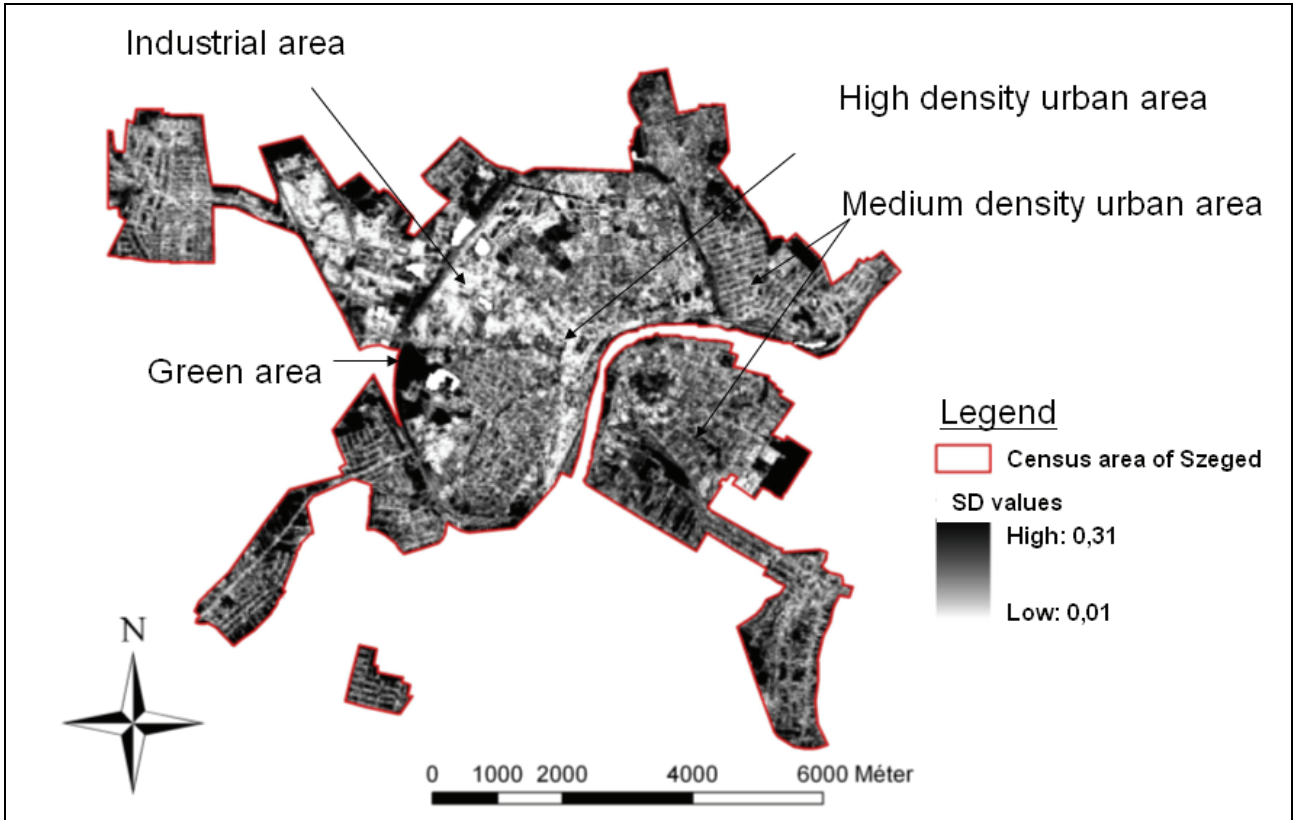


Figure 3. Standard deviation map made of 8 NDVI images from the time series of 1986

The visible relation between NDVI deviation values and the built-up density was verified with statistical analysis. The validation of the deviation map was achieved based on a Landsat TM satellite image from 24th July 1987. On these images we created a rate map with the method of the Spectral Mixture Analysis (SMA). This map shows the rate of vegetation, soil and artificial surface inside the pixel. The aim of SMA is to define the ratio of land cover types with homogeneous spectrum, the so-called endmembers inside the pixel [Roberts et al., 1998].

We applied the method of Normalized Spectral Mixture Analysis (NSMA) [Wu, 2004], in which we selected three endmembers: artificial surface, vegetation and soil.

$$\bar{R}_b = \frac{R_b}{\mu} \times 100$$

where

$$\mu = \frac{1}{N} \sum_{b=1}^N R_b$$

and \bar{R}_b is the normalized reflectance of band 'b' per pixel; R_b is the original reflectance of band 'b'; μ is the mean of reflectance values in the pixel; and N is the number of bands (6 at TM images).

The result of NSMA is a map that shows the rate of land cover types inside the pixel. These maps illustrate the spatial distribution of certain land cover types. Pixel values are between 0 and 1. In case of 1, the rate of the land cover type is 100 % inside the pixel (Figure 4). There is also a map that contains error values of the operation.

In the course of the validation we compared the subpixel rate map of artificial surfaces given as a result of SMA with the corresponding pixel values of the deviation map. We created cells by aggregating 3·3 pixels (90·90 m²) for the comparison to check the result. We supervised 289 pieces of these cells for a better cognition of the relations.

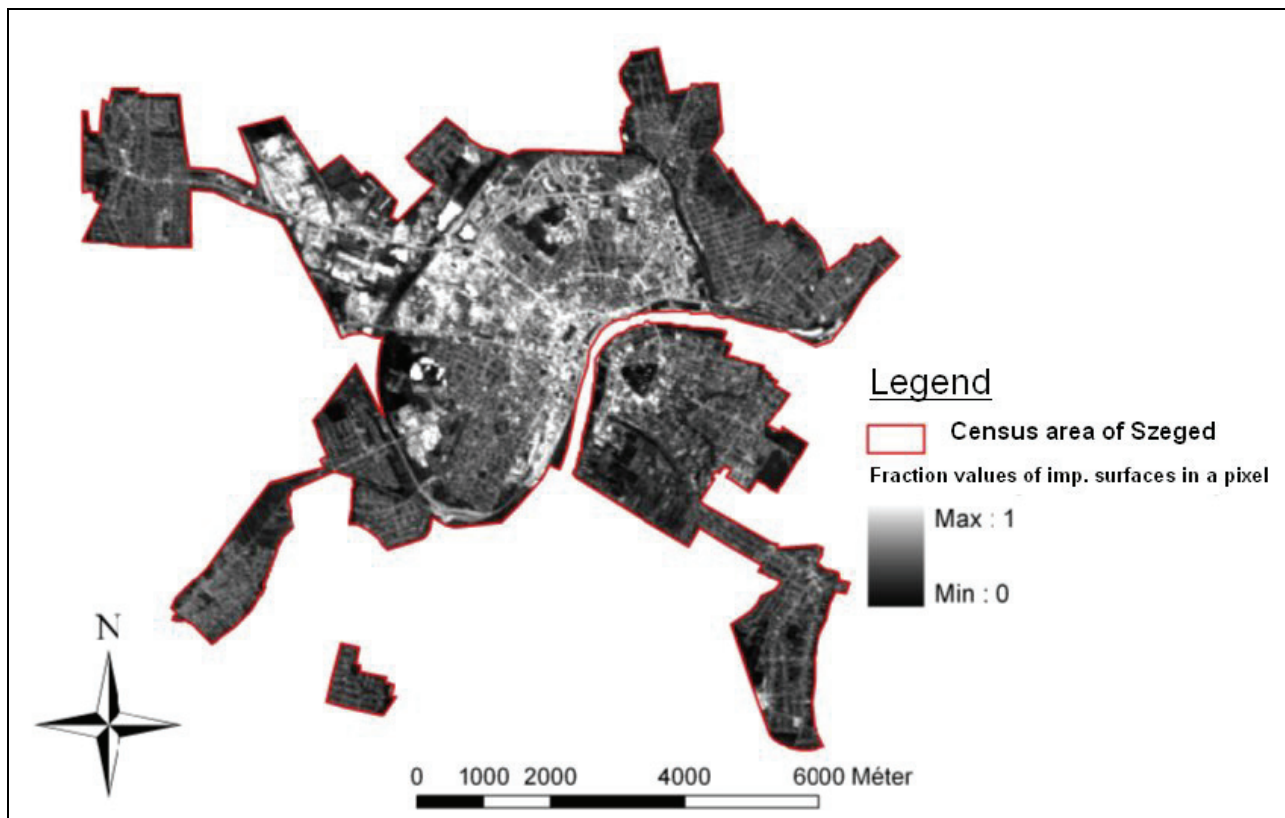


Figure 4. Fraction rate map of artificial surface taken from the spectral partition of a Landsat TM satellite image (24th July 1987)

For describing the regularity between these two attributes we used the method of regression analysis. An advantage of regression is that in the domain of the independent variable (x) we can estimate the most possibly appropriate y value for each x according to the sample. Figure 5 shows the diagram of the regression referring to the deviation of artificial surface. It has the following equation:

$$y = (10,6 - 58,2 \cdot x)^2,$$

where y: percentage of artificial surface (0-100); x: deviation calculated from NDVI values.

The correlation coefficient that indicates the strength of the relation has the value of -0,89. That means that there is a significant negative relationship between the two factors so that smaller rate of artificial surface belongs to higher NDVI deviation values.

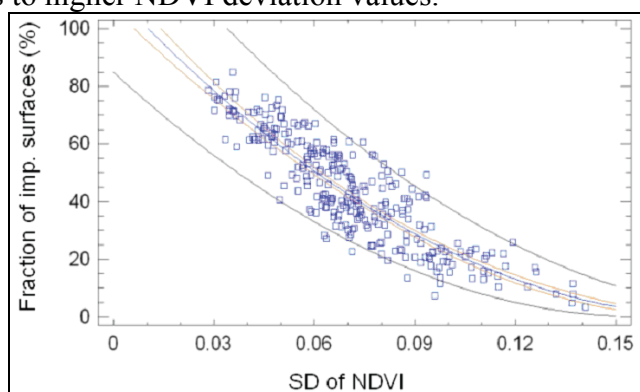


Figure 5. Relation between the standard deviation of NDVI values and the rate of artificial surface

After establishing the relation between artificial surface and NDVI deviation, we created the rate map of artificial surface from the produced deviation map using the equation of regression

(Figure 6). Using a simple, executable model each pixel values of the deviation map were substituted into the equation $y = (10,6 - 58,2x)^2$.

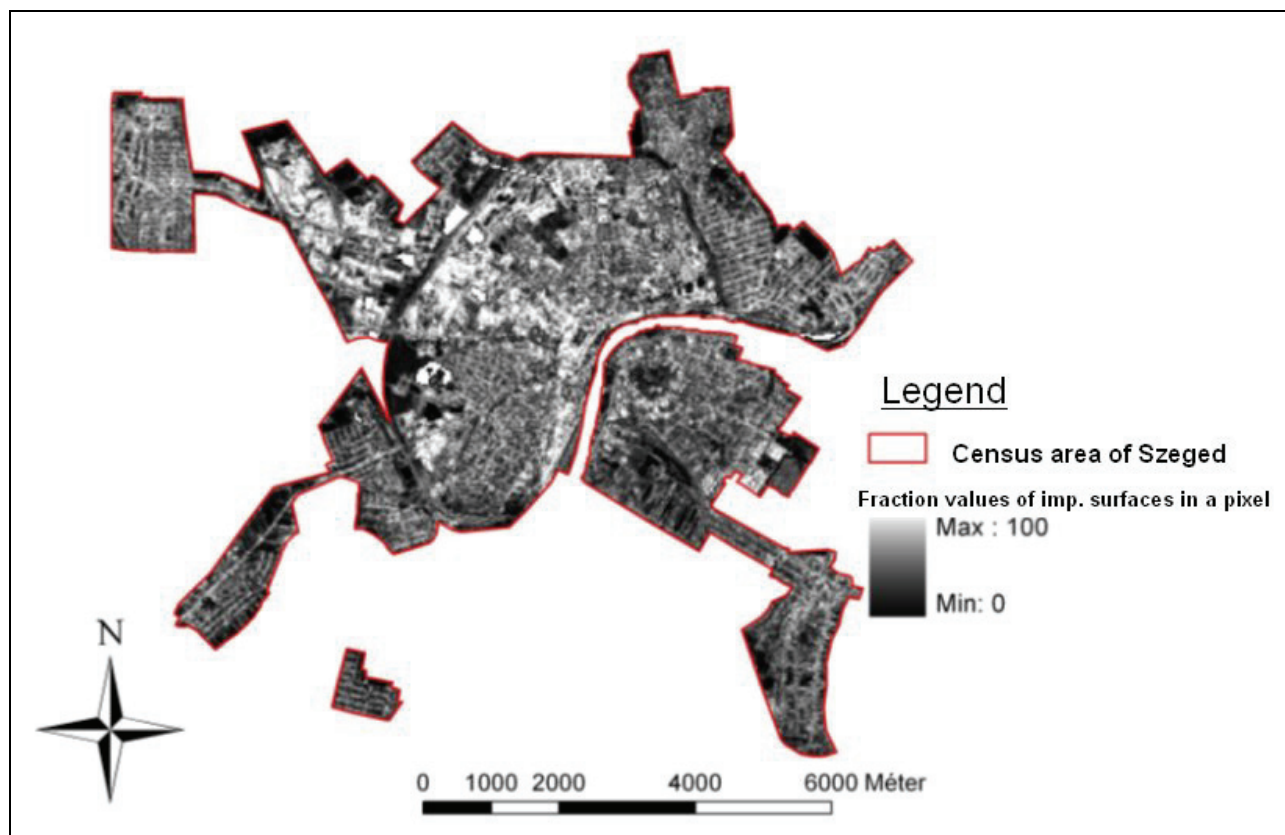


Figure 6. Fraction map of artificial surface calculated from the deviation map

A former developed statistical model was used to reconstruct the spatial distribution of urban heat island in 1986. In 1999 and 2000 not only the one-year period was investigated, but within this period we distinguished the so called heating (between 16 October and 15 April) and non-heating (between 16 April and 15 October) seasons.

It can be seen in Figure 7, that built-up density has a significant influence on the spatial patterns of the mean maximum UHI intensity (which is at 4 hours after sunset as supposed). The most obvious common features of these patterns are that the isotherms show almost regular concentric shapes with values increasing from the outskirts toward the inner urban areas. A vigorous deviation from this concentric shape occurs in the north-eastern part of the city, where the isotherms stretch toward the suburbs. This can be explained by the influence of the large housing estates with tall concrete buildings located mainly in the north-eastern part of the city with a built-up ratio higher than 75%.

In the non-heating season, the spreading out of the isolines of 2.25°C and 2.5°C to the north-west of the centre, and the isolines of 1.5°C and 1.75°C to the south-west are also caused by the high built-up ratio of more than 75% (Figure 6). The highest differences (more than 2.75°C) are concentrated in the densely built-up city centre (>75%) covered by about 8 grid cells (2 km²). The greatest intensity (3.18°C) is to the north of the central grid cell (C) in an adjacent cell. The mean maximum UHI intensity of higher than 2°C relatively large compared to the size of the study area. It covers about 40 grid cells (10 km²), which is about 37% of the investigated area.

The maximum UHI intensity (ΔT) can be described as a function of build up ratio (B) with the best fit regression line in the non heating period of the year (from April to October) with the following equation:

$$\Delta T = 0,018B + 0,716$$

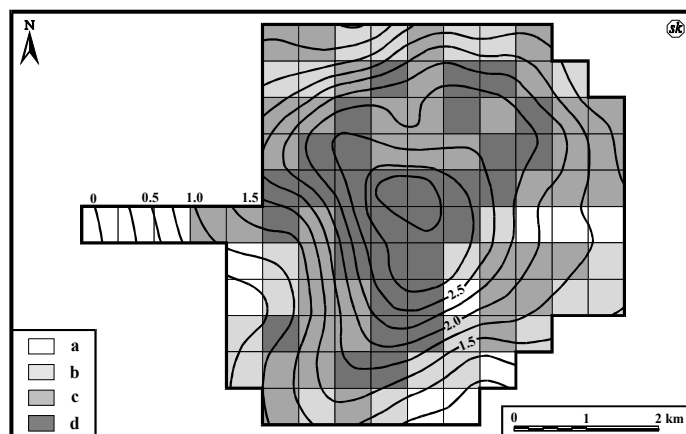


Figure 7 Spatial distribution of the mean maximum UHI intensity (°C) during the non-heating season (16 April - 15 October) in Szeged

According to this numerical the spatial distribution of average maximum UHI intensity values was calculated in the study area for the non-heating season and mapped by isolines in Fig. 8.

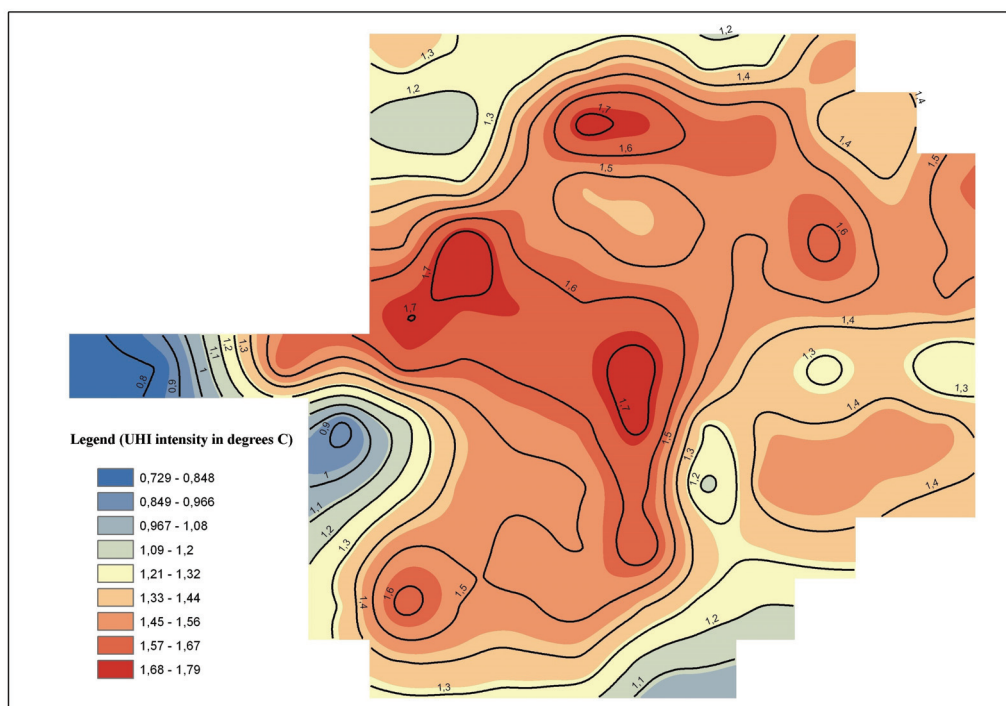


Figure 8. Spatial distribution of average maximum UHI intensity values in the non-heating season in 1986

3. Conclusions

On the basis of our research we can claim that medium resolution satellite images are suitable for mapping urban land cover based on the time series analysis of NDVI values, when unclouded satellite images are available in due frequency from the growing season of the year. Transforming the single images' intensity values per pixel into reflectance enables us to compare and analyse statistically our sequential images in a time series analysis. We demonstrated that NDVI standard deviation values, calculated from NDVI values per pixel, are in significant negative correlation with the rate of artificial surface inside the pixel. According to the equation of regression, NDVI standard deviation values can be calculated into the percentage values of the artificial surface, so spatial dif-

ferences of built-up density can be analysed inside the settlements. Hereby NDVI standard deviation value might be an appropriate input parameter in an urban climate model, for modelling urban heat island intensity out of heating season.

References

- [1] Bruzzone, L.–Smits, P.C. –Tilton, J.C. (2003): Foreword special issue on analysis of multitemporal remote sensing images, *IEEE Transactions on Geoscience and Remote Sensing* 41, 2419–2422.
- [2] Carlson, T.N. –Gillies, R.R. –Perry, E.M. (1994): A method to make use of thermal infrared temperature and NDVI measurements to infer surface soil water content and fractional vegetation cover, *Remote Sensing Reviews* 9, pp. 161–173.
- [3] Carlson, T.N.–Ripley, D.A. (1997): On the relation between NDVI, fractional vegetation cover, and leaf area index, *Remote Sensing of Environment* 62, pp. 241–252.
- [4] Chander, G. –Markham, B.L. (2003): Revised Landsat-5 TM Radiometric Calibration Procedures, and Post-Calibration Dynamic Ranges, *IEEE Transactions on Geoscience and Remote Sensing*, 41(11), 2674–2677.
- [5] Chavez, P.S., jr. (1996): Image-based atmospheric corrections - Revisited and Improved. *Photogrammetric Engineering and Remote Sensing* 62 (9), 1025-1036.
- [6] Gallo, K.P.–McNab, A.L.–Karl, T.R.–Brown, J.F.–Hood J.J.–Tarpley, J.D. (1993): The use of NOAA AVHRR data for assessment of the urban heat island effect, *Journal of Applied Meteorology* 32 (5), pp. 899–908.
- [7] Gillies, R.R.–Carlson, T.N. (1995): Thermal remote sensing of surface soil water content with partial vegetation cover for incorporation into climate models, *Journal of Applied Meteorology* 34, pp. 745–756.
- [8] Gillies, R.R.–Carlson, T.N.–Cui, J. Kustas, W.P.– Humes, K.S. (1997): A verification of the ‘triangle’ method for obtaining surface soil water content and energy fluxes from remote measurements of the Normalized Difference Vegetation Index (NDVI) and surface radiant temperature, *International Journal of Remote Sensing* 18, pp. 3145–3166.
- [9] Hall-Beyer M. (2003): Comparison of single-year and multiyear NDVI time series principal components in cold temperate biomes, *IEEE Transactions on Geoscience and Remote Sensing* 41, 2568–2574.
- [10] Henits, L. (2007). Városi felszínborítás vizsgálata ürfelvételekkel, OTDK dolgozat, Szeged, kézirat, p. 55.
- [11] Leprieux, C.–Kerr, Y.H.–Mastorchio, S.–Meunier, J.C. (2000): Monitoring vegetation cover across semi-arid regions: Comparison of remote observations from various scales. *International Journal of Remote Sensing*, 21, 281–300.
- [12] Liu, H.–Huete, A.R. (1995): A feedback based modification of the NDVI to minimize canopy background and atmospheric noise. *IEEE Transactions on Geoscience and Remote Sensing*, 33, 457–465.
- [13] Mezősi, G. –Mucsi, L. (1994): Urban density and expansion study using GIS and RS methods EGIS94 Paris Proceedings vol.II. pp. 1354-1363.
- [14] Moran, M.S.–Jackson R.D. –Slater P.N.–Teillet. P.M. (1992): Evaluation of simplified procedures for retrieval of land surface reflectance factors from satellite sensor output. *Remote Sensing of Environment* 41,169-184.
- [15] Mucsi, L.–Kovács, F.–Henits, L.–Tobak, Z.– van Leeuwen, B.–Szatmári, J. –Mészáros, M. (2007): Városi területhasználat és felszínborítás vizsgálata távérzékeléses módszerekkel, *Földrajzi tanulmányok* Vol. 1, Városökológia pp.:19-42, JATEPress
- [16] Owen, T.W.–Carlson T.N.– Gillies, R.R. (1998): An assessment of satellite remotely-sensed land cover parameters in quantitatively describing the climatic effect of urbanization, *International Journal of Remote Sensing* 19, pp. 1663–1681.
- [17] Pettorelli, N. –Vik, J.O.–Mysterud, A.–Gaillard, J.M.–Tucker C.J.–Stenseth, N.C. (2005): Using the satellite-derived NDVI to assess ecological responses to environmental change, *Trends in Ecology and Evolution* 20, 503–510.
- [18] Roberts, D.A.–Gardner, M.–Church, R.–Ustin, S.–Scheer, G.–Green, R.O. (1998): Mapping chaparral in the Santa Monica Mountains using multiple endmember spectral mixture models, *Remote Sensing of Environment* 65 pp. 267–279.
- [19] Unger, J., 1999: Urban-rural air humidity differences in Szeged, Hungary. *Int. J. Climatology* 19, 1509-1515.
- [20] [Unger, J.–Sümegehy, Z.–Gulyás, Á.–Bottyán, Zs.–Mucsi, L., 2001: Land-use and meteorological aspects of the urban heat island. *Meteorological Applications* 8, 189-194](#)
- [21] Wu, C. (2004): Normalized spectral mixture analysis for monitoring urban composition using ETM+ imagery, *Remote Sensing of Environment*, 93(4), 480-492.
- [22] Weng, Q.–Lu, D.–Schubring, J. (2004): Estimation of land surface temperature–vegetation abundance relationship for urban heat island studies, *Remote Sensing of Environment* 89, pp. 467–483.

